Journal of Materials Chemistry A

RSC Publishing

PAPER

View Article Online
View Journal | View Issue

Cite this: J. Mater. Chem. A, 2013, 1, 14206

Aminothermal synthesis of CHA-type SAPO molecular sieves and their catalytic performance in methanol to olefins (MTO) reaction†

Dong Fan,[abc] Peng Tian,[ab] Xiong Su,[abc] Yangyang Yuan,[abc] Dehua Wang,[abc] Chan Wang,[abc] Miao Yang,[ab] Linying Wang,[ab] Shutao Xu[ab] and Zhongmin Liu*[ab]

Received 22nd July 2013
Accepted 18th September 2013

DOI: 10.1039/c3ta12829f

www.rsc.org/MaterialsA

Aminothermal synthesis of SAPO molecular sieves, in which organic amines are used as both solvent and template, is explored based on a variety of amines. Di-iso-propylamine (DIPA) and *N*,*N*,*N*′,*N*′-tetramethylethylenediamine (TMEDA) are found to lead to the rapid crystallization of SAPO-34 with high solid yield. A solid yield of 96.2% could be acquired using the TMEDA system (200 °C, 12 h), which is the highest value ever reported for SAPO molecular sieves. SAPO-44 is obtained for the first time using the hexamethyleneimine (HMI) template. Detailed synthetic investigation shows that the silicon content in the initial gel has an important effect on the crystalline nature of the final products, and higher Si concentration favours the synthesis of pure SAPO-34 and SAPO-44. In addition, it is shown that the Si coordination environment in the samples is closely related to the choice of template. Among the three samples investigated, SAPO-34-DIPA has the lowest threshold of Si content for the formation of Si islands in the framework due to the smallest charge compensation centers occluded in its CHA cage. The catalytic performance of the synthesized samples is tested by the MTO reaction and a high olefin selectivity of 85.8% is obtained on SAPO-34 templated by DIPA.

1 Introduction

Silicoaluminophosphate (SAPO) molecular sieves were firstly reported by Union Carbide in 1984.[1,2] The structures of SAPOs cover a range of different structure types; some are analogous to certain zeolites such as SAPO-34 (CHA topology), but a large number have unique structures without a zeolite counterpart. Among SAPOs, small-pore SAPO-34 has received great attention in recent years due to its good performance in methanol-to-olefins (MTO) reaction.[3,4] The CHA framework topology, comprised of cylinder-like cages (6.7 × 6.7 × 10.0 Å) with 8-ring openings (3.8 × 3.8 Å), has been reported to be the ideal breeding ground for hydrocarbon pool intermediates (polymethylbenzenes as active species) in the MTO reaction.[5–9] Recently, a commercial MTO process with a production capacity of 600 000 tons of light olefins per year has been successfully put into operation based on the SAPO-34 catalyst.[10]

The traditional synthesis of SAPO-34 is commonly carried out in a hydrothermal way, which involves the addition of large amounts of water as the mass and heat transfer medium. The presence of organic amines as structure directing agents (SDAs) or templates is essential for the successful synthesis.[11,12] Many organic amines, including tetraethylammonium hydroxide (TEAOH),[1,2] dipropylamine,[2] isopropylamine,[13] piperidine,[14] morpholine,[15] triethylamine (TEA),[4] and diethylamine (DEA),[16,17] *etc.*, have been reported to direct the crystallization of SAPO-34. According to the literature, the choice of SDAs for the synthesis of SAPO-34 is crucial for the properties of the final products, such as microscopic structures, elemental compositions and morphologies. For example, Barthomeuf *et al.*[18] carried out comparative studies on the properties of SAPO-34 templated by TEAOH and morpholine, and concluded that the template could determine the maximum charge and govern the distribution of silicon in the framework. The same group also reported that the choice of template exerted a significant impact on the short- and long-term stability of SAPO-34.[19] Gon *et al.*[20] and Nishiyama *et al.*[21] found the crystallite size variation of SAPO-34 crystals synthesized using different templates, respectively, and successfully correlated this with their catalytic performance in the MTO reaction. Our group systematically studied the synthesis of SAPO-34 templated by DEA and discovered that DEA tended to prompt higher silicon incorporation into the SAPO-34 framework than TEAOH and TEA.[16]

Novel synthetic methods are always attractive in the field of molecular sieves, which may have the possibility to create new materials or known phases with specific properties.[22,23] One of

[a]Dalian National Laboratory for Clean Energy, Dalian Institute of Chemical Physics, Chinese Academy of Sciences, Dalian, P. R. China. E-mail: liuzm@dicp.ac.cn
[b]National Engineering Laboratory for Methanol to Olens, Dalian Institute of Chemical Physics, Chinese Academy of Sciences, Dalian, P. R. China
[c]University of Chinese Academy of Sciences, Beijing, P. R. China

† Electronic supplementary information (ESI) available. See DOI: 10.1039/c3ta12829f

the alternative synthetic methods for SAPO molecular sieves is the solvothermal synthesis.[24–26] The methodology was firstly introduced into the zeolite synthesis by Bibby and Dale, in which organic solvents instead of water were used as the reaction medium.[27] Xu and co-workers extended this method to the synthesis of aluminophosphate (AlPO) molecular sieves. By employing alcohols as solvents, they synthesized many novel AlPO materials with anionic frameworks, among which JDF-20 possessing 20-ring extra-large pores are the most attractive ones.[24,28,29] Recently, we have proposed a novel solvothermal approach to prepare SAPO molecular sieves, designated as aminothermal synthesis, in which the organic amine acts as both the template and solvent.[30] Solvothermal synthesis of SAPO-34 and SAPO-18 were realized for the first time with this method. The synthesized materials exhibited good adsorption capacities for CO_2 and high CO_2/CH_4 ratio. Moreover, the organic amines could be easily collected and recycled after each synthesis, suggesting the environmental benignity of the methodology. It should be noted that the aminothermal synthesis is not truly anhydrous, and the presence of small quantity of water in the initial system is essential for the successful crystallization of SAPO molecular sieves.

In the present work, a variety of organic amines were employed for the aminothermal synthesis of SAPO molecular sieves. The investigated organic amines include *n*-propylamine (PA), tri-*n*-propylamine (TPA), di-iso-propylamine (DIPA), *n*-butylamine (BA), *N*,*N*-dimethylbenzylamine (DMBA), 1,2-ethylenediamine (EDA), *N*,*N*,*N*′,*N*′-tetramethylethylenediamine (TMEDA), cyclohexylamine (CHA) and hexamethyleneimine (HMI). Three amines, TMEDA, DIPA and HMI, rarely used for the synthesis of CHA-type SAPO molecular sieves (termed as CHA-SAPO), are found to direct the formation of SAPO-34 and SAPO-44. Detailed investigations on the synthesis, physiochemical properties and catalytic performance of CHA-SAPO samples are carried out.

2 Experimental

2.1 General procedure of aminothermal synthesis

Organic amines (chemical pure) were used as received. Pseudoboehmite (70.5 wt%), phosphoric acid (85 wt%), and silica sol (27.5 wt%) were used as inorganic precursors.

The molar ratio of the initial gel is $R/Al_2O_3/P_2O_5/SiO_2/H_2O = X/1.2/0.9/0.5/14.6$, in which the volume of R is kept constant (50 ml), and the masses of Al, P and Si sources are 8.4 g, 10.4 g and 5.3 g, respectively. Water from each resource has been calculated into the gel composition. A typical synthesis procedure is as follows. Organic amine, pseudoboehmite, silica sol and water were added in sequence into a glass beaker. The mixture was stirred at room temperature for 5 min, and then transferred into a stainless steel autoclave. After further addition of phosphoric acid, the autoclave was sealed quickly, placed in an oven and rotated at 60 rpm for 20 min to get a homogeneous mixture. Subsequently, the autoclave was heated in 60 min to the desired temperature under rotation and kept for a certain time. The solid product was obtained after centrifugation, washing and drying at 100 °C overnight.

The solid yield of samples is calculated by the following formula: yield (%) = $(M_{sample} \times DW\%) \times 100/(M_{Al_2O_3} + M_{P_2O_5} + M_{SiO_2})_{gel}$, where M_{sample}, DW% and $(M_{Al_2O_3} + M_{P_2O_5} + M_{SiO_2})_{gel}$ stand for the weight of as-synthesized samples, the weight percentage of inorganic oxides in the as-synthesized samples derived from TG analysis, and the dry mass of the three oxides in the starting mixture, respectively.

2.2 Characterization

The powder XRD pattern was recorded on a PANalytical X'Pert PRO X-ray diffractometer with CuKα radiation ($\lambda = 1.54059$ Å), operating at 40 kV and 40 mA. The chemical composition of the solid samples was determined with a Philips Magix-601 X-ray fluorescence (XRF) spectrometer. The crystal morphology was observed by scanning electron microscopy (SEM, Hitachi S-3400N). All NMR experiments were performed on a Varian Infinity plus 400WB spectrometer with a BBO MAS probe operating at a magnetic field strength of 9.4 T. The resonance frequencies were 104.2, 161.9, 79.4, and 100.5 MHz for ^{27}Al, ^{31}P, ^{29}Si and ^{13}C, respectively. Chemical shifts were referenced to 1.0 M $Al(NO_3)_3$ for ^{27}Al, 85% H_3PO_4 for ^{31}P, and 2,2-dimethyl-2-ilapentane-5-sulfonate sodium salt (DSS) for ^{29}Si and ^{13}C. The spinning rates of the samples at the magic angle were 4, 10, 6 and 8 kHz for ^{29}Si, ^{27}Al, ^{31}P and ^{13}C, respectively. Textural properties of the calcined samples were determined by N_2 adsorption at 77 K on a Micromeritics ASAP 2020 system. The total surface area was calculated based on the BET equation. The micropore volume and micropore surface area were evaluated using the *t*-plot method. TG and DSC analysis were performed on a TA SDTQ600 analyzer with the temperature-programmed rate of 10 °C min^{-1} under an air flow of 100 ml min^{-1}. The temperature-programmed desorption of ammonia (NH_3-TPD) experiments were conducted in a Micromeritics Autochem II 2920 device. 0.2 grams of the sample particles (40–60 mesh) were loaded into a U-quartz tube and pretreated at 650 °C for 60 min under helium flow. After cooling down to 100 °C, a gas mixture of NH_3 and He flow was introduced to saturate the sample surface with NH_3 adsorption (60 min). After this, He flow was purged through the sample for 30 min to remove the weakly adsorbed NH_3 molecules. The measurement of the desorbed NH_3 was performed from 100 °C to 700 °C (10 °C min^{-1}) under He flow (20 ml min^{-1}).

2.3 Catalyst evaluation

MTO reaction was carried out with a fixed-bed reactor at atmospheric pressure. 1.2 grams of the calcined sample (40–60 mesh) were loaded into the reactor. The catalyst was pretreated in a flow of nitrogen atmosphere at 550 °C for 1 h. Nitrogen flow was turned off when the reactor was cooled down to 450 °C. A mixture of methanol and water with a CH_3OH–H_2O weight ratio of 40/60 was consequently pumped into the reactor. The weight hourly space velocity (WHSV) of methanol was 2 h^{-1}. The products were analysed by an Agilent GC7890 gas chromatograph equipped with an FID detector and Poraplot Q-HT capillary column.

The methanol conversion is defined as the percentage of CH_3OH consumed during the MTO reaction. The selectivity is defined as the weight percent of each compound in the total products. It should be noted that dimethylether (DME) is considered as a reactant instead of a product here.

3 Results and discussion

3.1 Aminothermal synthesis of SAPO molecular sieves based on a variety of organic amines

Fig. 1 displays the XRD patterns of the as-synthesized samples prepared with different amines as both the solvent and template. It was found that primary amines, including BA, CHA, PA and EDA, mainly led to the formation of lamellar materials (a–d, Fig. 1). SAPO-5 was obtained as the final product while employing TPA or DMBA amines (e and f, Fig. 1). Three amines, including HMI, DIPA and TMEDA, were found to direct the crystallization of SAPO molecular sieves with the CHA topology (g–i, Fig. 1). It should be noted that the samples templated by DIPA and TMEDA exhibit the typical diffraction pattern of SAPO-34, while some difference is observed for the sample templated by HMI. The distance between two peaks in the range of 23–26° (2 theta) and the relative intensities of the neighboring peaks around 30° (2 theta) in the pattern of SAPO-HMI sample obviously differ from those of SAPO-34-DIPA and SAPO-34-TMEDA, suggesting that SAPO-HMI was in fact SAPO-44, a silicoaluminophosphate also possessing chabasite topology.[31]

Among the three organic amines for CHA-SAPO molecular sieves, DIPA was once reported for the dry-gel synthesis of SAPO-34.[32] Although TMEDA has been patented to direct the formation of SAPO-34,[33] the hydrothermal synthesis was conducted *via* a fluoride route. Without F^-, the product would become SAPO/AlPO-21. Moreover, Pastore *et al.*[34] reported that the lamellar AlPO-kanemite precursor could be transformed into CHA-SAPO (designated as CAL-1 therein) by a hydrothermal reaction with silica in the presence of HMI. Their results showed that the synthesis of CAL-1 was restricted within a relatively narrow initial SiO_2/Al_2O_3 ratio (0.8–1.2), and CAL-1 was actually co-templated by HMI and BA (the SDA for the AlPO-kanemite). To the best of our knowledge, there is no research on SAPO-44 templated by HMI until now.

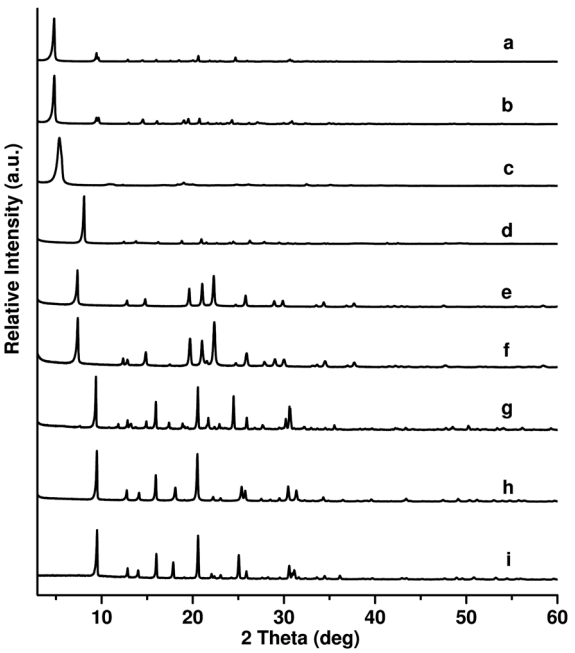

Fig. 1 XRD patterns of the as-synthesized samples using BA (a), CHA (b), PA (c), EDA (d), TPA (e), DMBA (f), HMI (g), DIPA (h) and TMEDA (i) as the solvent and template. The crystallization conditions are 200 °C and 48 h for all except for sample i (200 °C, 12 h). The peak intensities of samples a–d shown in the figure have been reduced to 1/3 of the original.

3.2 Synthesis of SAPO-34 with DIPA as the solvent and template

The effect of silicon content in the initial gel on the synthesis was firstly investigated based on the DIPA system by fixing other synthetic conditions. The results are shown in Table 1. AlPO-11 instead of AlPO-34 was acquired as the final product in the absence of silicon. This is not surprising because DIPA is a well-known template for the hydrothermal synthesis of AlPO-11. On the other hand, AlPO-34 could only crystallize in a fluoride-containing system. By increasing the $x(SiO_2)$ to 0.15, SAPO-34 appeared together with small quantity of SAPO-11 as impurity. Pure SAPO-34 was readily synthesized when the silicon content reached 0.3 or higher. However, a small amount of the amorphous phase due to the unreacted silica residues started to appear in the product when the $x(SiO_2)$ became 1.0, implying the capacity limitation of silicon incorporation into the framework of SAPO-34-DIPA. The elemental composition of the obtained samples was determined by XRF and shown in Table 1. The Si concentration in SAPO-34 rises with the increasing content in the initial gel, though the Si incorporation degree shows a decline.

The crystallization process of SAPO-34 using DIPA as the solvent and template was studied based on sample 4 (Table 1). The process exhibits a feature of fast crystallization. The relative crystallinity of the product reaches 87% after a crystallization duration of 3 hours. This value further increases to 96.9% after 7 hours and keeps at a high level until the end of the crystallization. The Si content in the product shows an increasing trend with time, consistent with what we have found in the hydrothermal synthesis of SAPO-34 templated by TEA and DEA.[17,35] It implies that both the initial Si content in the gel and the crystallization time can modify the Si concentration in the final product. Moreover, the solid yield during the crystallization shows a maximum of 90.1% at $t = 12$ h. Afterwards, it gradually drops and a yield of 83.8% is obtained for the 48 h sample.[36] The possible reason is that molecular sieves are generally metastable materials, which crystallize through a kinetic control. Dissolution and phase transformation might occur after the optimal synthesis period of a certain phase.

The SEM images (Fig. 2) reveal that SAPO-34-DIPA crystals (samples 4 and 9) possess the typical rhombohedral morphology. The crystal size ranges from 1 to 2 μm. The N_2 physisorption results of samples 3 and 4 are given in Table 2. Both samples exhibit a BET surface area of around 590 $m^2\ g^{-1}$

Table 1 The influence of synthetic parameters on the synthesis results based on the DIPA system

Sample[a]	$x(SiO_2)$	t (h)	Product	Product composition	Si incorporation[b]	Relative crystallinity[c] (%)	Yield (%)
1	0	48	AlPO-11	—	—	—	—
2	0.15	48	SAPO-34 + SAPO-11	—	—	—	—
3	0.3	48	SAPO-34	$Al_{0.511}P_{0.416}Si_{0.073}$	1.09	—	92.3
4	0.5	48	SAPO-34	$Al_{0.482}P_{0.422}Si_{0.096}$	0.91	100	83.8
5	0.75	48	SAPO-34	$Al_{0.490}P_{0.389}Si_{0.121}$	0.80	—	87.3
6	1.0	48	SAPO-34 + amorphous SiO_2	$Al_{0.458}P_{0.357}Si_{0.185}$	—	—	93.0
7	0.5	3	SAPO-34	$Al_{0.516}P_{0.413}Si_{0.071}$	0.67	87.0	61.8
8	0.5	7	SAPO-34	$Al_{0.507}P_{0.409}Si_{0.084}$	0.79	96.9	84.7
9	0.5	12	SAPO-34	$Al_{0.501}P_{0.407}Si_{0.092}$	0.87	97.3	90.1

[a] All samples are prepared using 50 ml of DIPA as both the solvent and template under a crystallization temperature of 200 °C. The initial molar composition for the inorganic species is as follows: $Al_2O_3/P_2O_5/SiO_2/H_2O = 1.2/0.9/x(SiO_2)/14.6$. [b] The silicon incorporation is defined as $[Si/(Si + Al + P)]_{product}/[Si/(Si + Al + P)]_{gel}$. [c] The relative crystallinity is calculated based on the relative intensity of the three strongest peaks (2θ = 9.5, 16.0 and 20.5°) in the XRD patterns.

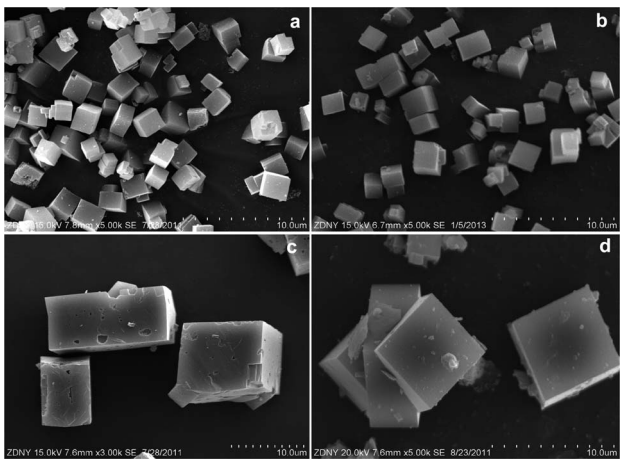

Fig. 2 SEM images of the as-synthesized samples 4(a), 9(b), 13(c), 18(d).

Table 2 Textural properties of the samples

	Surface area ($m^2\ g^{-1}$)		Pore volume ($cm^3\ g^{-1}$)		
Sample	S_{total}[a]	S_{micro}[b]	S_{ext}[c]	V_{total}	V_{micro}[d]
3	587	586	1	0.27	0.27
4	590	587	3	0.30	0.27
13	503	490	13	0.24	0.23
18	490	466	24	0.24	0.22

[a] BET surface area. [b] t-plot micropore surface area. [c] t-plot external surface area. [d] t-plot micropore volume.

and a micropore volume of 0.27 $cm^3\ g^{-1}$. Both the SEM image and N_2 physisorption results verify the high purity and crystallinity of the SAPO-34 templated by DIPA.

3.3 Synthesis of SAPO-34 with TMEDA as the solvent and template

The effect of the silicon content on the synthesis using TMEDA as the solvent and template are summarized in Table 3. It was found that AlPO-21 possessing the AWO topology was crystallized from the silica-free initial gel. By increasing the $x(SiO_2)$ to 0.15, SAPO-34 appeared together with the presence of a large amount of SAPO-21. After further increasing the value to 0.30, SAPO-34 became the dominant product at the expense of SAPO-21. Pure SAPO-34 could be obtained in the range of 0.5–1.0. It should be mentioned that high solid yields of SAPO-34 are observed under the present aminothermal environment, especially for sample 13, which shows a value of 96.2%. Such a high yield has never been reported before for SAPO molecular sieves.

The crystals of SAPO-34-TMEDA (sample 13) present elongated rhombohedron morphology with a relatively large crystal size of around 10 μm (Fig. 2). The BET surface area and micropore volume of sample 13 were calculated to be 503 $m^2\ g^{-1}$ and 0.23 $cm^3\ g^{-1}$, respectively. The values are lower than those of SAPO-34-DIPA, but still in the reasonable range for SAPO-34, indicating the good crystallinity of the product synthesized under the TMEDA system.

3.4 Synthesis of SAPO-44 with HMI as the solvent and template

Synthetic results based on the aminothermal synthesis of SAPO-44 with HMI as the solvent and template verify again that the Si content in the starting gel has great effect on the final product (Table 3). In the silica-free system, aluminophosphate with an unknown phase was acquired. When the value of $x(SiO_2)$ was 0.3 or higher, SAPO-44 was obtained as the crystalline phase. Noteworthily, samples 17 and 18 possess larger silicon contents than SAPO-34-DIPA and SAPO-34-TMEDA synthesized from the same initial gel composition, suggesting that HMI is able to induce higher silicon incorporation into the framework of SAPO-44 (see the column of Si incorporation in Tables 1 and 3). However, the solid yield with HMI system is unexpectedly low (~40%).

By shortening the crystallization duration to 12 h, no crystalline product was obtained. This phenomenon indicates that the crystallization kinetic under the HMI system is much slower than that under DIPA and TMEDA systems, suggesting the weaker templating efficacy of HMI in the synthesis of SAPO-44.

Table 3 The influence of synthetic parameters on the synthesis results based on TMEDA and HMI systems

Sample[a]	Amine	$x(SiO_2)$	t (h)	Product	Product composition	Si incorporation[b]	Yield (%)
10	TMEDA	0	12	AlPO-21	—	—	43.2
11	TMEDA	0.15	12	SAPO-21 + SAPO-34	—	—	47.5
12	TMEDA	0.30	12	SAPO-34 + minor SAPO-21	$Al_{0.521}P_{0.389}Si_{0.089}$	—	72.2
13	TMEDA	0.5	12	SAPO-34	$Al_{0.506}P_{0.381}Si_{0.112}$	1.05	96.2
14	TMEDA	0.75	12	SAPO-34	$Al_{0.488}P_{0.372}Si_{0.139}$	1.03	94.7
15	TMEDA	1.0	12	SAPO-34	$Al_{0.470}P_{0.351}Si_{0.179}$	0.96	89.8
16	HMI	0	48	Unknown phase	—	—	—
17	HMI	0.3	48	SAPO-44	$Al_{0.503}P_{0.388}Si_{0.109}$	1.63	41.4
18	HMI	0.5	48	SAPO-44	$Al_{0.507}P_{0.366}Si_{0.127}$	1.19	40.1
19	HMI	0.5	12	Amorphous	—	—	—

[a] All samples are prepared using 50 ml of organic amine as both the solvent and template under a crystallization temperature of 200 °C. The initial molar composition for the inorganic species is as follows: $Al_2O_3/P_2O_5/SiO_2/H_2O = 1.2/0.9/x(SiO_2)/14.6$. [b] The silicon incorporation is defined as $[Si/(Si + Al + P)]_{product}/[Si/(Si + Al + P)]_{gel}$.

This might also be the possible reason for the low solid yield associated with the HMI system.

The crystal morphology of SAPO-44 (sample 18) was also examined by SEM. It exhibits the typical rhombohedral shape. Moreover, it is found that the textural properties of sample 18 are close to those of SAPO-34-TMEDA. These results imply the good quality of SAPO-44 obtained under the HMI system.

3.5 Physiochemical properties of CHA-SAPOs synthesized with three templates: ^{13}C MAS NMR, TG-DSC, ^{29}Si, ^{27}Al and ^{27}P MAS NMR

The as-synthesized samples 4, 13 and 18 (SAPO-34-DIPA, SAPO-34-TMEDA and SAPO-44, respectively) were used for various characterizations.

^{13}C MAS NMR spectra were recorded in order to verify the exact template species occluded in the three samples (see Fig. 3). The spectrum of sample 4 exhibits two symmetrical peaks centred around 46 and 19 ppm, which are ascribed to the carbon atoms bound to the nitrogen atoms (C_1) and the methyl carbons (C_2) in the DIPA molecule, respectively. For sample 16 templated by the diamine TMEDA, the two peaks in the spectrum occur at relatively higher chemical shifts (58 ppm for C_1 and 47 ppm for C_2), due to the intimate connection of both methyl and methylene to the nitrogen atoms with stronger electronegativity. Sample 18, obtained under the HMI system, displays two resonance peaks centred around 49 and 26 ppm. The former peak was commonly ascribed to the carbon atoms (C_α) adjacent to the imino groups, while the latter one was assigned to the remaining carbon atoms (C_β and C_γ) in the HMI ring.[34] Generally, the obtained spectra are in good agreement with the previous literature, suggesting that the investigated three samples are well templated by DIPA, TMEDA and HMI, respectively.

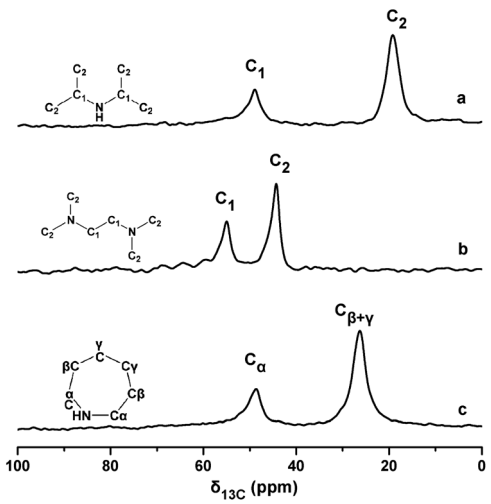

Fig. 3 ^{13}C MAS NMR of the as-synthesized samples 4(a), 13(b) and 18(c).

The TG and DSC curves for the three samples are illustrated in Fig. S1, S2 and S3, respectively (see ESI†). The weight loss in the samples occurs in three or four stages (Table 4). In the first stage (<230 °C), the weight loss is attributed to the water desorption. The second weight loss between 230 and 410 °C with an exothermal process is due to the combustion decomposition of the template. The third and fourth weight losses at a temperature higher than 410 °C with strongly exothermic processes are likely associated with the further removal of organic residue occluded in the channels and cages of samples. In addition, it can be seen from the curves that there is no weight loss and exothermic peak associated with structural collapse until 900 °C, suggesting the high thermal stability of SAPO-34 and SAPO-44 synthesized in the present work. Notably, sample 18 demonstrated a much obvious weight loss due to the template removal, indicating a higher organic occlusion of HMI

Table 4 Thermal analysis results of the samples

Sample	Weight loss (wt%)			Template per cage
	I	II	III + IV	
4	4.3	10.8	1.0	1.01
13	3.2	6.3	6.5	0.96
18	3.5	4.0	15.7	1.91

molecules in the SAPO-44 framework. Based on the elemental composition and topological structure of the sample, it is calculated that for samples 4 and 13, one organic amine molecule could be accommodated per CHA cage. As for sample 18, every cage contains nearly two HMI molecules, possibly due to the relatively small size of HMI.

Solid-state ^{29}Si, ^{31}P and ^{27}Al MAS NMR spectra were recorded to investigate the local atomic coordination environments in the as-synthesized samples. Fig. 4 presents the ^{29}Si spectra of the three samples. Only one symmetric peak centred at −91 ppm, ascribed to Si (4Al) species, appears in the spectrum of SAPO-34-TMEDA. Complex Si environments are observed for SAPO-34-DIPA and SAPO-44. Besides the apparent resonance at −91 ppm, there emerge several small signals at around −96, −100, −105 and −110 ppm, corresponding to Si (3Al), Si (2Al), Si (1Al) and Si-island, respectively. Additionally, a weak peak at −85 ppm is also present in the spectra of both samples, which possibly arises from the $Si(OAl)_3(OH)$ or $Si(OAl)(OSi)(OH)_2$ species located in the Si–Al domains.[37,38] According to the deconvoluted analysis of the spectra (Table S1†), the concentration of Si (4Al) species in the three samples has the following order: SAPO-34-TMEDA > SAPO-44 > SAPO-34-DIPA. Barthomeuf *et al.*[18] once reported that a higher template number per cage in SAPO-34 could lead to a larger framework charge, and thus a higher Si (4Al) concentration in the framework. In the present work, the template number per cage for TMEDA, HMI and DIPA are 1, 2 and 1, respectively. However, it should be noted that TMEDA, containing two nitrogen atoms, actually has two charge compensation centers despite only one molecule is accommodated in a cage. Therefore, the smallest charge compensation centers confined in the cage of SAPO-34-DIPA causes the lowest Si (4Al) concentration in the framework, though it possesses the lowest Si content among the three investigated samples.

As shown in Fig. 5, two peaks centred at around 37 and 9 ppm are observed in the ^{27}Al MAS NMR spectra of the two SAPO-34 samples. The strong resonance at high field should arise from tetrahedral Al species, whereas the weak one is attributed to penta-coordinated Al formed by an additional interaction of one water or template molecule with the framework aluminum. For SAPO-44, one more peak centred at 0 ppm is observed besides the two peaks shown in the spectra of SAPO-34 samples, which corresponds to hexa-coordinated aluminum. The assignment is confirmed by the ^{27}Al spectrum of the calcined SAPO-44, in which only one signal with a chemical shift of 37 ppm appears.

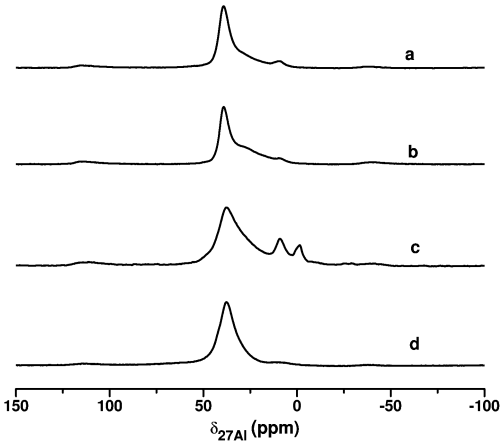

Fig. 5 ^{27}Al MAS NMR of the as-synthesized samples 4(a), 13(b), 18(c) and calcined sample 18(d).

The ^{31}P MAS NMR spectra of the samples are illustrated in Fig. 6. One strong resonance peak at −30 ppm appears in the spectra of all three samples, suggesting the predominant P (4Al) environment in the framework. In addition, the spectrum of SAPO-44 demonstrates two additional small peaks located at −17.6 and −11.4 ppm, which might be assigned to partially hydrated $P(OAl)_x(OH)_y$ species.[39]

3.6 Catalytic performance in the MTO reaction

Among the three serial CHA-SAPO molecular sieves, samples 3, 13 and 17 (SAPO-34-DIPA, SAPO-34-TMEDA and SAPO-44) with pure CHA structure and low Si contents were selected to test

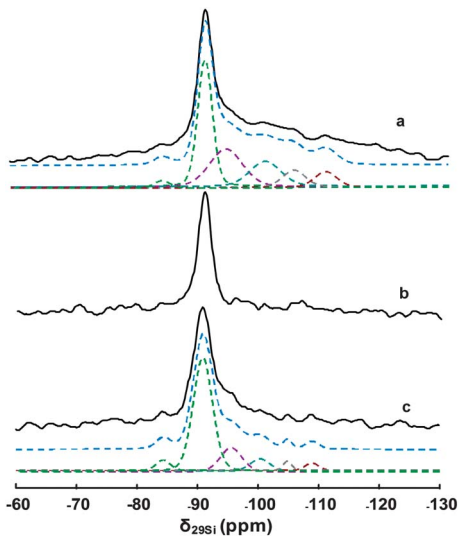

Fig. 4 ^{29}Si MAS NMR of the as-synthesized samples 4(a), 13(b) and 18(c).

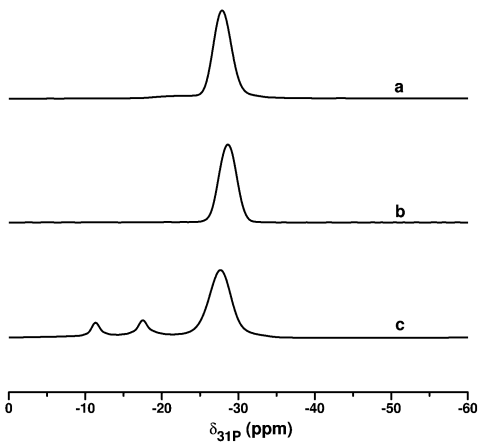

Fig. 6 ^{31}P MAS NMR of the as-synthesized samples 4(a), 13(b) and 18(c).

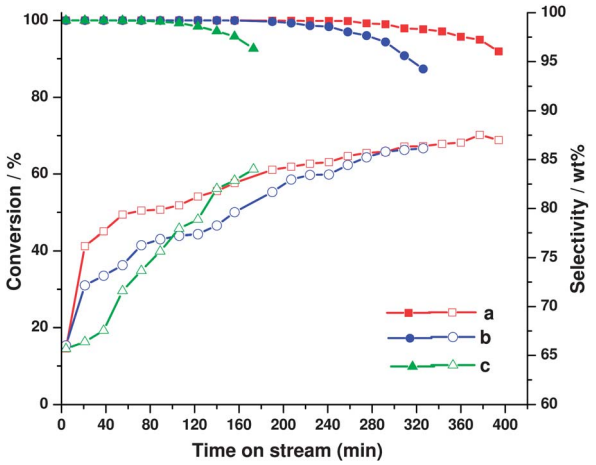

Fig. 7 Methanol conversion (solid) and selectivity of C_2H_4 plus C_3H_6 (hollow) during the MTO reaction on samples 3 (a), 13 (b), and 17 (c) (*reaction conditions*: 450 °C, CH_3OH_3 WHSV = 2 h^{-1}, 40 wt% methanol solution).

their catalytic properties in the MTO reaction, considering that SAPO-34 with lower Si contents generally exhibited better MTO performance.[3,40] The results are illustrated in Fig. 7 and Table S2.†

Both SAPO-34 samples demonstrate good catalytic properties, especially for SAPO-34 templated by DIPA. The selectivity of ethylene and propylene on SAPO-34-DIPA could reach 85.8% under complete methanol conversion. NH_3-TPD experiments are carried out to probe the acid properties of the two samples and the curves are given in Fig. S4.† Clearly, sample 13 possesses larger acid concentration and higher acid strength than sample 3. According to the literature, SAPO-34 with lower Si content (lower acidity) generally has better MTO catalytic performance.[41,42] It is therefore inferred that the larger amount of strong/moderate acid sites in sample 13 prompts the occurrence of side reactions such as coking and hydrogen transfer (higher propane selectivity), and causes a lower selectivity to light olefins and shorter catalyst lifetime. Moreover, the larger surface area and higher pore volume with sample 3 would also benefit its catalytic stability.

SAPO-44 exhibits the worst catalytic performance, whatever be the lifetime and selectivity to light olefins. This is in agreement with the previous results.[43] The difference between the microstructures of SAPO-44 and SAPO-34, as reflected in their XRD patterns, is supposed to be responsible for the bad catalytic behaviour of SAPO-44.

4 Conclusions

Three SAPO molecular sieves with the CHA topology have been aminothermally synthesized with DIPA, TMEDA and HMI templates, respectively. Both DIPA and TMEDA were found to direct the formation of SAPO-34 with a fast crystallization rate and high solid yield. 90% and 96.2% yields have been achieved after 12 h crystallization based on DIPA and TMEDA systems, respectively. Pure SAPO-44 was obtained in the HMI system. This is the first synthesis report on SAPO-44 using HMI as the template. Among the three amines, HMI shows a relatively high ability to prompt the silicon incorporation into the framework of SAPO-44. Moreover, the concentration of Si (4Al) species in the three samples has the following order: SAPO-34-TMEDA > SAPO-44 > SAPO-34-DIPA. According to the TG results, the smallest number of charge compensation centers confined in the CHA cage of SAPO-34-DIPA results in the lowest Si (4Al) content in the framework. MTO evaluation results reveal that SAPO-34-DIPA possesses excellent catalytic properties. The selectivity of ethylene and propylene on SAPO-34-DIPA could reach as high as 85.8% under the investigated conditions. It is believed that the excellent MTO performance together with the high synthetic yield will promote the aminothermal synthesis of SAPO-34-DIPA to be an interesting method for preparing the MTO catalyst.

Acknowledgements

The authors would like to acknowledge the National Natural Science Foundation of China (Grant no. 21101150 and Grant no. 21103180) for the support of this project. Dong Fan acknowledges the financial support of DNL-Topsøe scholarship provided by Haldor Topsøe Corporation.

Notes and references

1 B. M. Lok, C. A. Messina, R. L. Patton, R. T. Gajek, T. R. Cannan and E. M. Flanigen, *J. Am. Chem. Soc.*, 1984, **106**, 6092–6093.
2 B. M. Lok, C. A. Messina, R. L. Patton, R. T. Gajek, T. R. Cannan and E. M. Flanigen, *US Pat.* 4440871, 1984.
3 S. Wilson and P. Barger, *Microporous Mesoporous Mater.*, 1999, **29**, 117–126.
4 J. Liang, H. Y. Li, S. Zhao, W. G. Guo, R. H. Wang and M. L. Ying, *Appl. Catal.*, 1990, **64**, 31–40.
5 I. M. Dahl and S. Kolboe, *J. Catal.*, 1994, **149**, 458–464.
6 W. G. Song, H. Fu and J. F. Haw, *J. Am. Chem. Soc.*, 2001, **123**, 4749–4754.
7 W. G. Song, H. Fu and J. F. Haw, *J. Phys. Chem. B*, 2001, **105**, 12839–12843.
8 W. G. Song, J. F. Haw, J. B. Nicholas and C. S. Heneghan, *J. Am. Chem. Soc.*, 2000, **122**, 10726–10727.
9 J. Z. Li, Y. X. Wei, J. R. Chen, P. Tian, X. Su, S. T. Xu, Y. Qi, Q. Y. Wang, Y. Zhou, Y. L. He and Z. M. Liu, *J. Am. Chem. Soc.*, 2012, **134**, 836–839.
10 http://www.syn.ac.cn/english/index.php.
11 D. W. Lewis, C. R. A. Catlow and J. M. Thomas, *Chem. Mater.*, 1996, **8**, 1112–1118.
12 D. W. Lewis, C. M. Freeman and C. R. A. Catlow, *J. Phys. Chem.*, 1995, **99**, 11194–11202.
13 N. Rajic, D. Stojakovic, S. Hocevar and V. Kaucic, *Zeolites*, 1993, **13**, 384–387.
14 E. Dumitriu, A. Azzouz, V. Hulea, D. Lutic and H. Kessler, *Microporous Mater.*, 1997, **10**, 1–12.
15 A. M. Prakash and S. Unnikrishnan, *J. Chem. Soc., Faraday Trans.*, 1994, **90**, 2291–2296.

16 G. Liu, P. Tian, J. Li, D. Zhang, F. Zhou and Z. Liu, *Microporous Mesoporous Mater.*, 2008, **111**, 143–149.
17 G. Y. Liu, P. Tian, Y. Zhang, J. Z. Li, L. Xu, S. H. Meng and Z. M. Liu, *Microporous Mesoporous Mater.*, 2008, **114**, 416–423.
18 R. Vomscheid, M. Briend, M. J. Peltre, P. P. Man and D. Barthomeuf, *J. Phys. Chem.*, 1994, **98**, 9614–9618.
19 M. Briend, R. Vomscheid, M. J. Peltre, P. P. Man and D. Barthomeuf, *J. Phys. Chem.*, 1995, **99**, 8270–8276.
20 K. Y. Lee, H. J. Chae, S. Y. Jeong and G. Seo, *Appl. Catal., A*, 2009, **369**, 60–66.
21 N. Nishiyama, M. Kawaguchi, Y. Hirota, D. Van Vu, Y. Egashira and K. Ueyama, *Appl. Catal., A*, 2009, **362**, 193–199.
22 R. E. Morris and S. J. Weigel, *Chem. Soc. Rev.*, 1997, **26**, 309–317.
23 Y. Jin, Q. Sun, G. Qi, C. Yang, J. Xu, F. Chen, X. Meng, F. Deng and F.-S. Xiao, *Angew. Chem.*, 2013, **125**, 9342–9345.
24 Q. S. Huo and R. R. Xu, *J. Chem. Soc., Chem. Commun.*, 1990, 783–784.
25 A. K. Sinha and S. Seelan, *Appl. Catal., A*, 2004, **270**, 245–252.
26 N. Venkatathri, *Catal. Commun.*, 2006, **7**, 773–777.
27 D. M. Bibby and M. P. Dale, *Nature*, 1985, **317**, 157–158.
28 Q. H. Huo, R. R. Xu, S. G. Li, Z. G. Ma, J. M. Thomas, R. H. Jones and A. M. Chippindale, *J. Chem. Soc., Chem. Commun.*, 1992, 875–876.
29 R. H. Jones, J. M. Thomas, J. S. Chen, R. R. Xu, Q. S. Huo, S. G. Li, Z. G. Ma and A. M. Chippindale, *J. Solid State Chem.*, 1993, **102**, 204–208.
30 D. Fan, P. Tian, S. Xu, Q. Xia, X. Su, L. Zhang, Y. Zhang, Y. He and Z. Liu, *J. Mater. Chem.*, 2012, **22**, 6568.
31 S. Ashtekar, S. V. V. Chilukuri and D. K. Chakrabarty, *J. Phys. Chem.*, 1994, **98**, 4878–4883.
32 L. Zhang, J. Yao, C. Zeng and N. Xu, *Chem. Commun.*, 2003, 2232.
33 K. G. Strohmaier and P. Murry, *US Pat.* 6835363B1, 2004.
34 H. O. Pastore, E. C. de Oliveira, G. B. Superti, G. Gatti and L. Marchese, *J. Phys. Chem. C*, 2007, **111**, 3116–3129.
35 L. Xu, A. P. Du, Y. X. Wei, Y. L. Wang, Z. X. Yu, Y. L. He, X. Z. Zhang and Z. M. Liu, *Microporous Mesoporous Mater.*, 2008, **115**, 332–337.
36 Synthesis for sample 4 and 9 have been repeated twice. Similar product yields are obtained as shown in Table 1.
37 C. Doremieux-Morin, C. Martin, J.-M. Bregeault and J. Fraissard, *Appl. Catal.*, 1991, **77**, 149–161.
38 L. Zhang, J. Bates, D. H. Chen, H. Y. Nie and Y. N. Huang, *J. Phys. Chem. C*, 2011, **115**, 22309–22319.
39 B. Chen and Y. Huang, *J. Phys. Chem. C*, 2007, **111**, 15236–15243.
40 A. Izadbakhsh, F. Farhadi, F. Khorasheh, S. Sahebdelfar, M. Asadi and Y. Z. Feng, *Appl. Catal., A*, 2009, **364**, 48–56.
41 U. Olsbye, S. Svelle, M. Bjrgen, P. Beato, T. V. W. Janssens, F. Joensen, S. Bordiga and K. P. Lillerud, *Angew. Chem., Int. Ed.*, 2012, **51**, 5810–5831.
42 L.-T. Yuen, S. I. Zones, T. V. Harris, E. J. Gallegos and A. Auroux, *Microporous Mater.*, 1994, **2**, 105–117.
43 J. S. Chen and J. M. Thomas, *Catal. Lett.*, 1991, **11**, 199–207.